Updates on the Two Habit Model Optical Property Database: Full Resolution and Improvements Compared to Previously Developed Databases

James Coy, Masanori Saito, Jiachen Ding, Tong Ren, Ping Yang

Texas A&M University, Department of Atmospheric Sciences

CERES Meeting May 11-13 2021

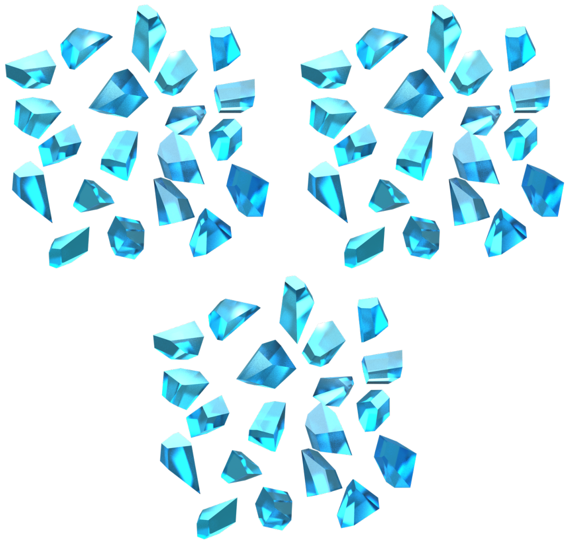

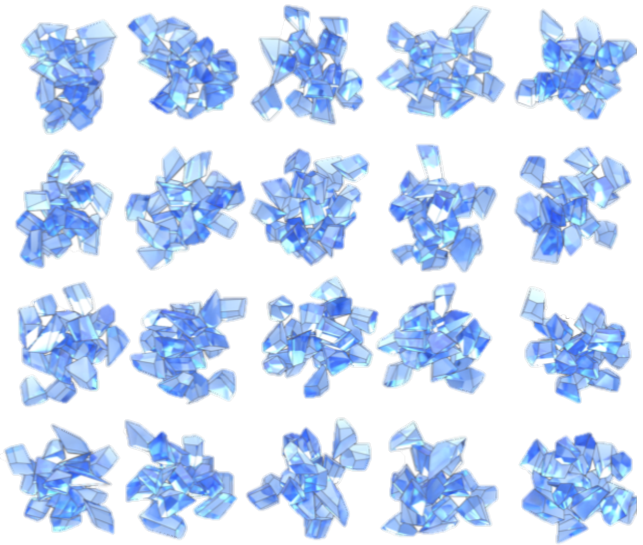

Importance of Ice Cloud Particle Models

- Ice cloud properties still least understood atmospheric parameters in remote sensing and radiative transfer calculations due to uncertainties in ice cloud microphysical and optical properties.
- Ice cloud particle models help to describe microphysical (e.g., particle habit) and optical properties (e.g., scattering phase matrix) of ice clouds.
    - These properties are fundamental to applications in remote sensing, radiative transfer, and general circulation models.
    - New ice cloud particle models being developed/improved upon to provide more accurate downstream calculations.

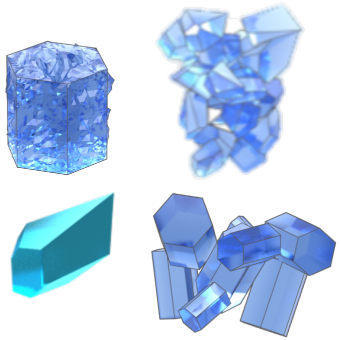

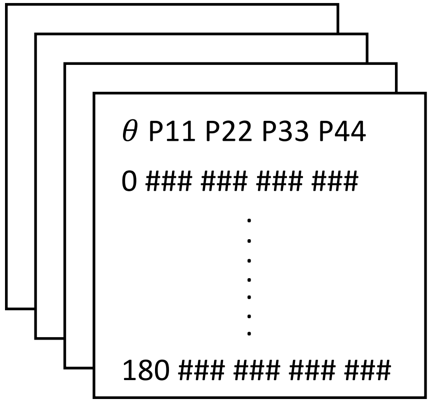

Loeb et al., 2018

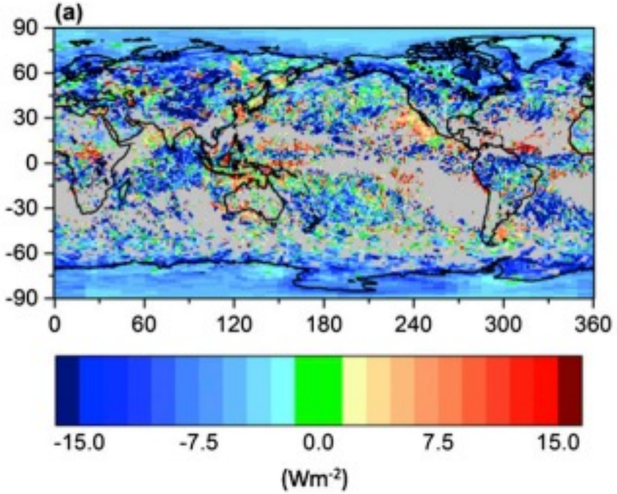

Reasons for a new Two-Habit Model Database

- Observations of ice particles that comprises ice clouds show that particles can be irregularly shaped rather than being idealized such as a hexagonal column.
- Conventional particle size classification of maximum dimension do not represent irregular particle shapes leading to physical and optical inconsistency.
- Previously developed Two-Habit Model databases lack accurate backscattering which is important for applications for lidar-based radiative transfer simulations.

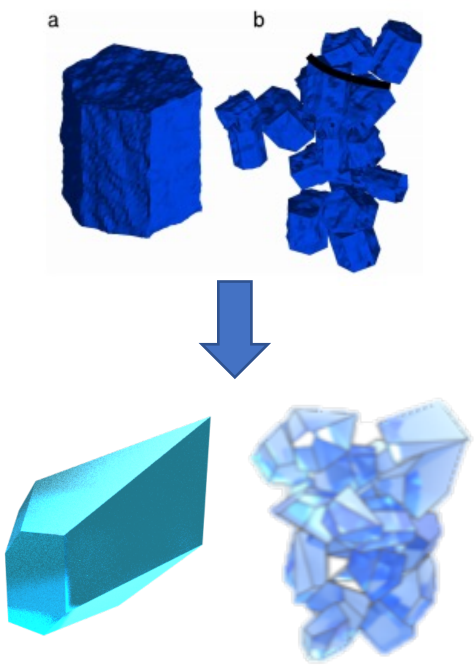

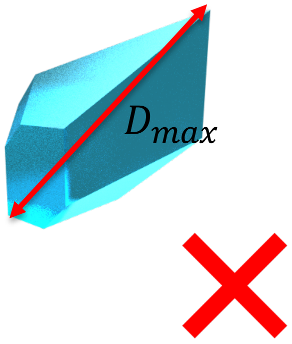

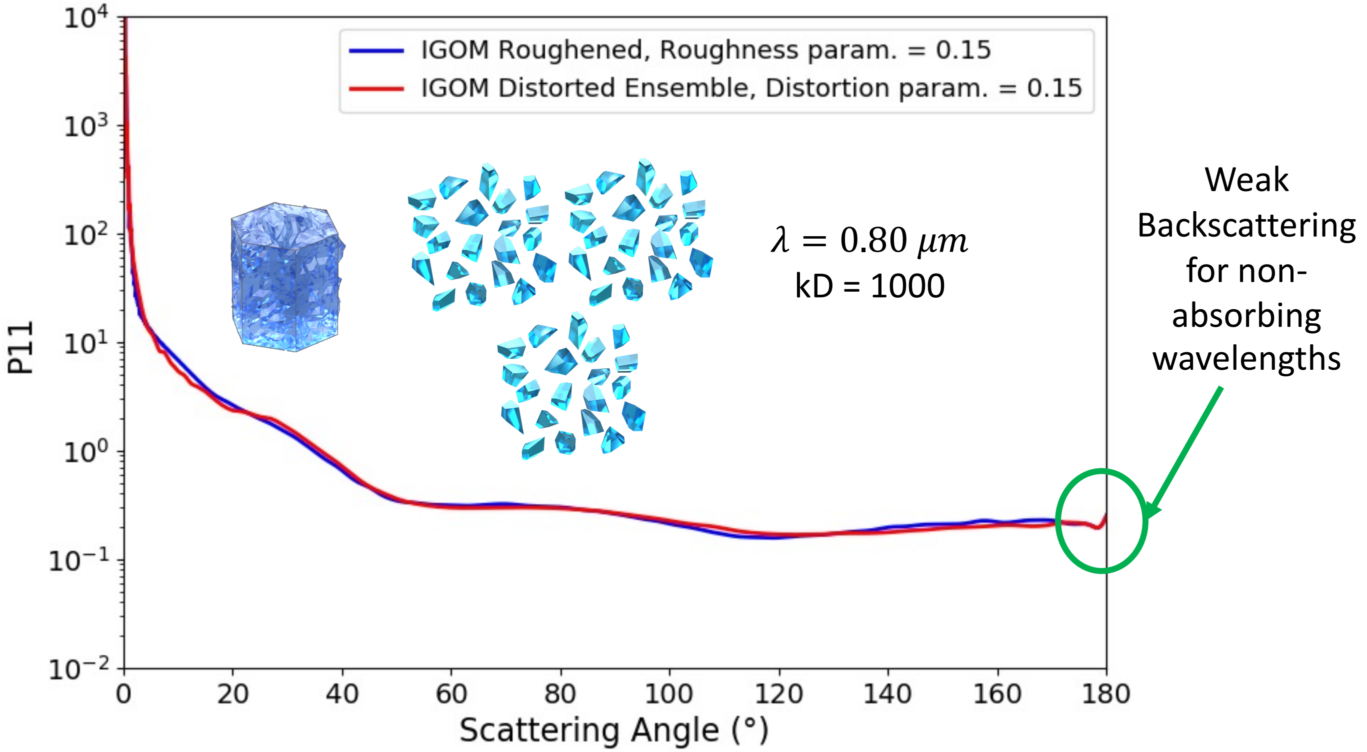

Reasons for a new Two-Habit Model Database

- The Two-Habit Model (THM) follows the Thompson et al. 2008 cloud ice scheme than other commonly used single-scattering databases.
- Improvements to the THM should maintain the consistency with the cloud ice scheme.

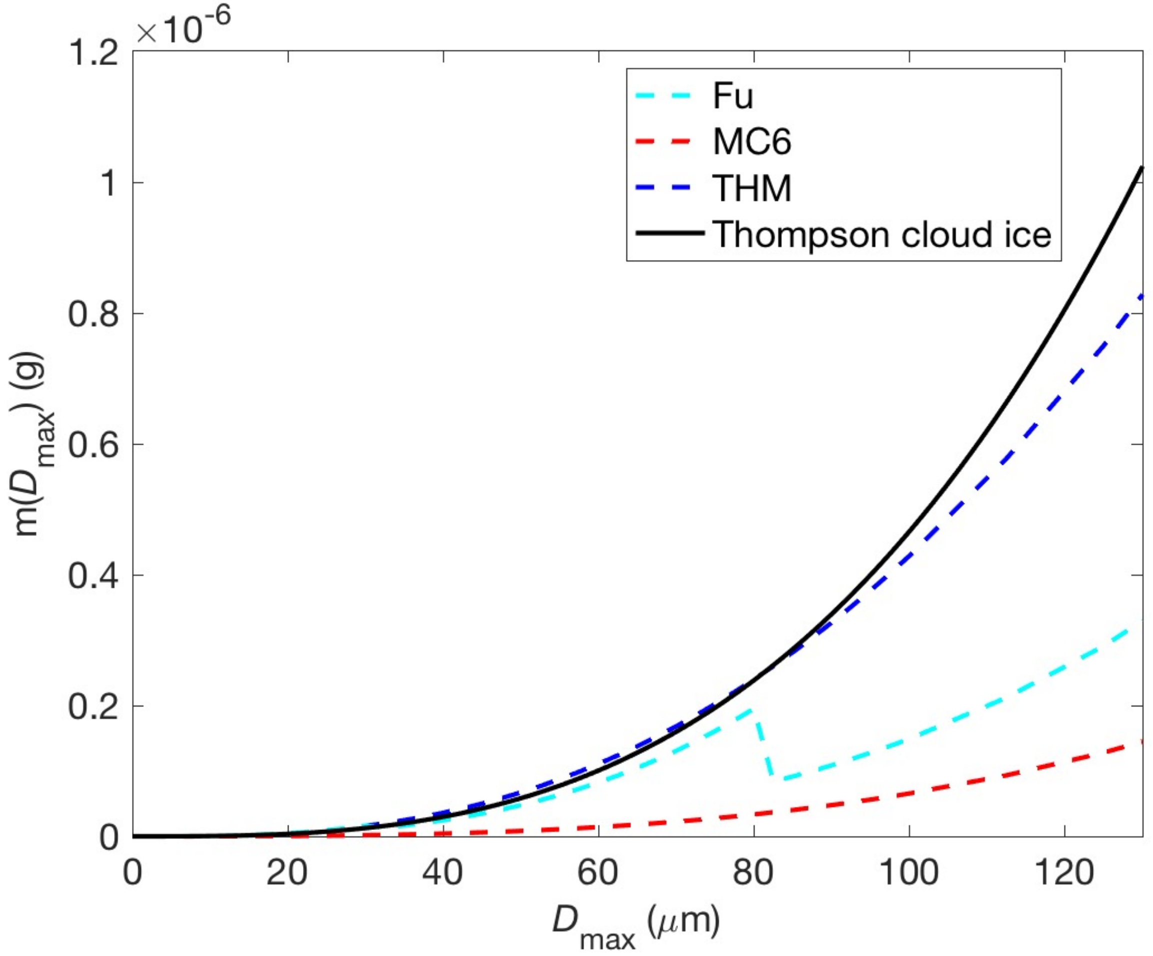

Recap: Preliminary New Two Habit Model

- Same size-dependent, and continuous mixing ratio as the last version THM (Loeb et al., 2018) (Figure 1a).
- New 60-particle ensemble of distorted single columns.
- Volume-projected area equivalent sphere diameter (D_{VA}) size characterization (Figure 1b).
- Physical Geometric Optics Model (PGOM)-based enhanced backscattering calculations applied to existing Improved Geometric Optics Model (IGOM) single-scattering calculations (Figure 1c).

1a

$$f_{single} = \begin{cases} e^{-0.005(D_{VA}-30)}, & D_{VA} \geq 30\mu m \\ 1, & D_{VA} < 30\mu m \end{cases}$$

$$f_{aggregate} = 1.0 - f_{single}$$

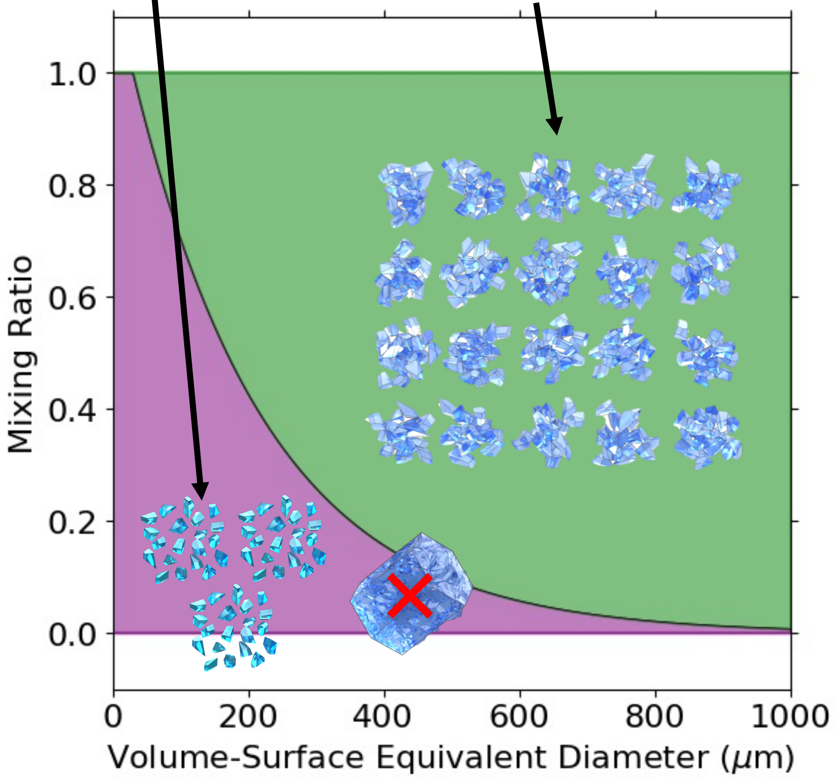

1b

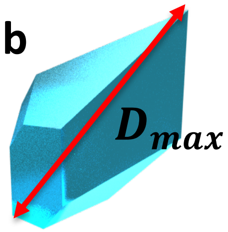

$$D_{VA} = \frac{3V}{2A_p}$$

V: Particle volume

A_p: Projected area

	Preliminary THM (Version 3)
Wavelength	42 bins (0.2 – 20 μm)
Size	59 bins (2.0 – 1000.0 μm)

1c

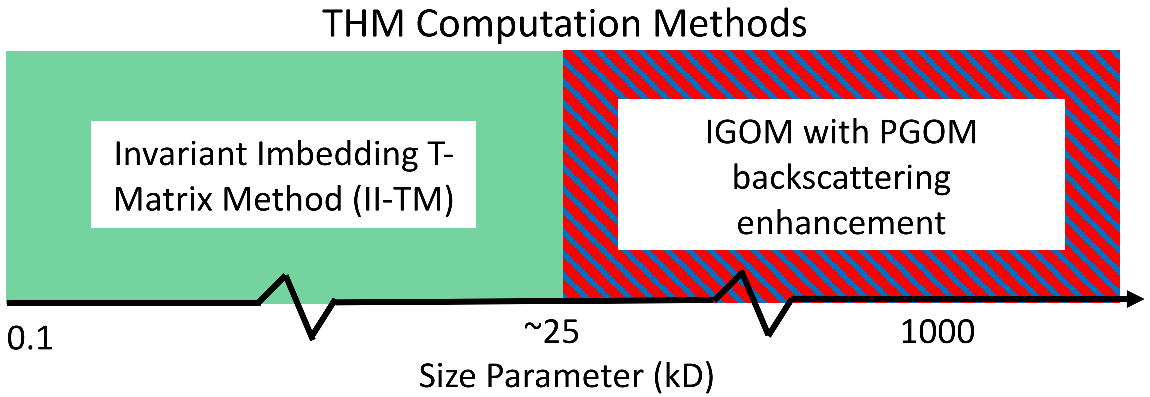

Recap: THM New Size Characterization

- Upon transitioning from roughened particle to distorted particle ensemble, D_{max} size characterization results in optical and physical inconsistency (Warren and Grenfell, 1999).
  - Particle distortion causes changes in particle volume and projected area.
- **3 other size characterizations** considered for replacing D_{max}.
  - Volume-projected area equivalent sphere diameter (D_{VA}) selected to replace D_{max} as new size characterization for new THM (Figure 2).

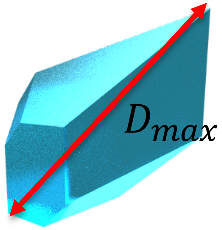

Surface Area-Equivalent Sphere Diameter

$$D_{sur} = \left(\frac{6}{\pi} S_{particle}\right)^{1/2}$$

Volume-Equivalent Sphere Diameter

$$D_{vol} = \left(\frac{6}{\pi} V_{particle}\right)^{1/3}$$

Volume/Projected Area-Equivalent Sphere Diameter

$$D_{VA} = \frac{3V_{particle}}{2A_{particle}}$$

2 Extinction Efficiency (Q_{ext}) Size Characterization Comparison

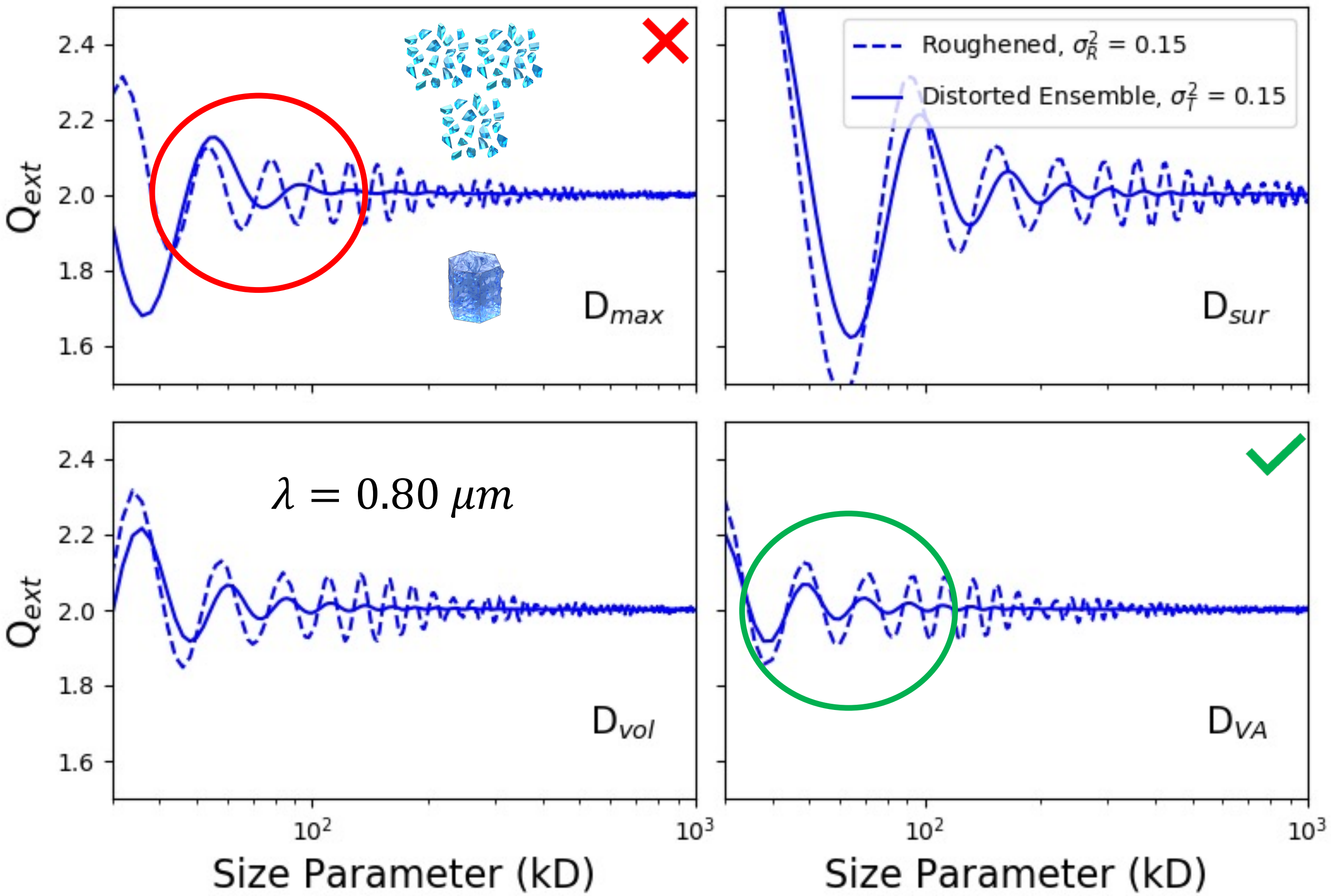

Recap: PGOM-Based Backscattering Enhancement

- PGOM provides accurate backscattering calculations but significantly more computationally demanding than IGOM and IITM.
  - PGOM fully considers the vector properties and phase difference characteristics of ice particles while IGOM summarizes it for faster computation time.
- The PGOM-based backscattering enhancement, calculated from lookup table from selected refractive indices and size parameters, was applied to the preliminary THM.

3a

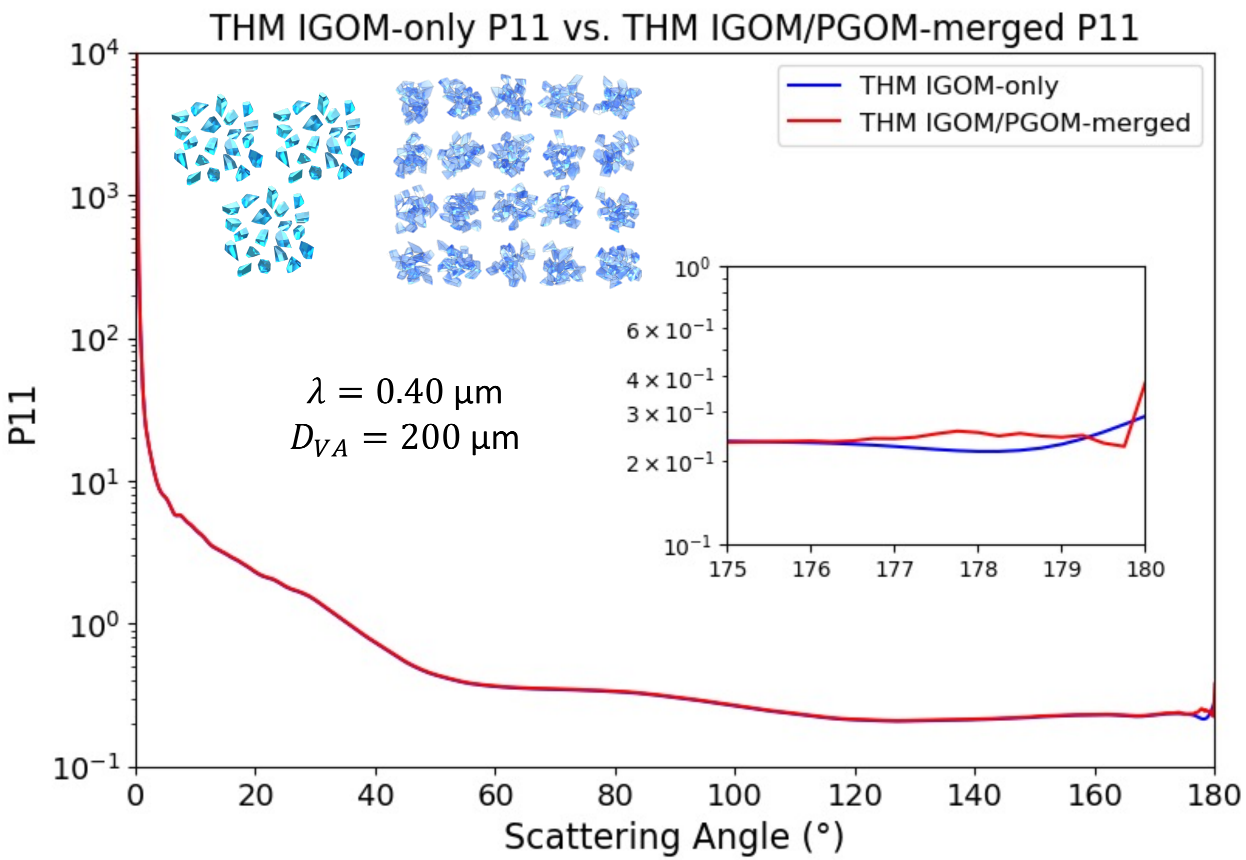

3b

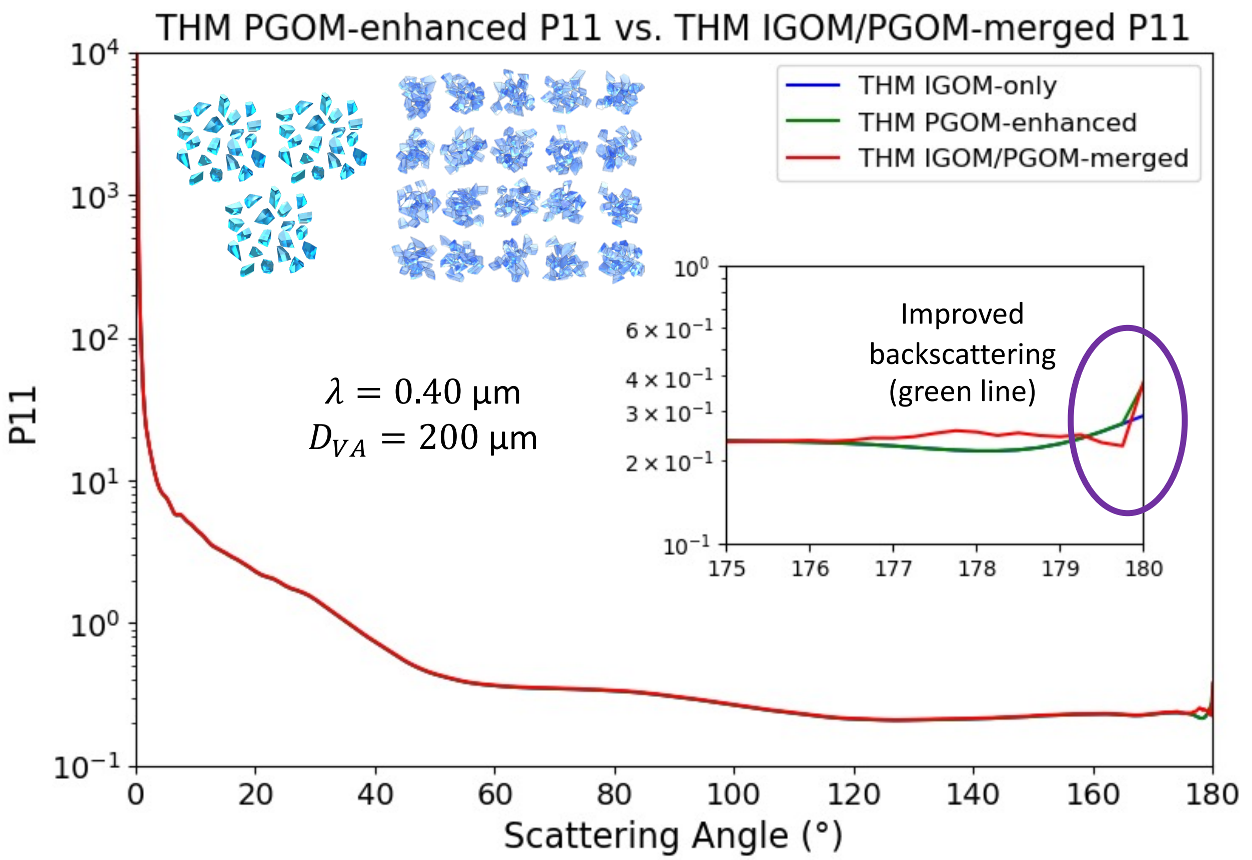

Recap: Major Changes in Lidar-based Radiative Transfer Simulations

- Conducted lidar-based radiative transfer simulations utilizing CALIOP/CALIPSO data and the cloud optical thickness (COT) – integrated attenuated backscattering (IAB) retrieval approach.
  - Validate changes in simulation results for non-absorbing wavelengths (532 nm) caused by using the new THM with enhanced backscattering.
- New Preliminary THM showed significantly higher IAB for larger effective radii and COT.
  - New THM reveals more COT information in the COT – IAB retrieval approach.

IAB-COT Retrieval Method
(Ding et al., 2016)

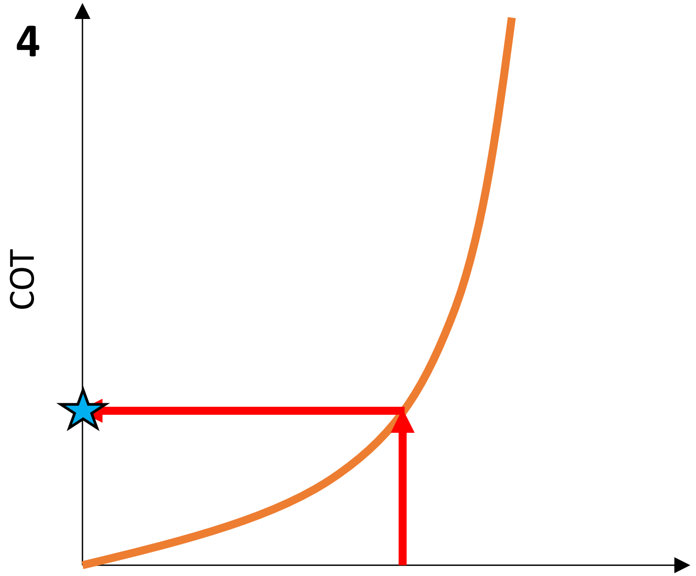

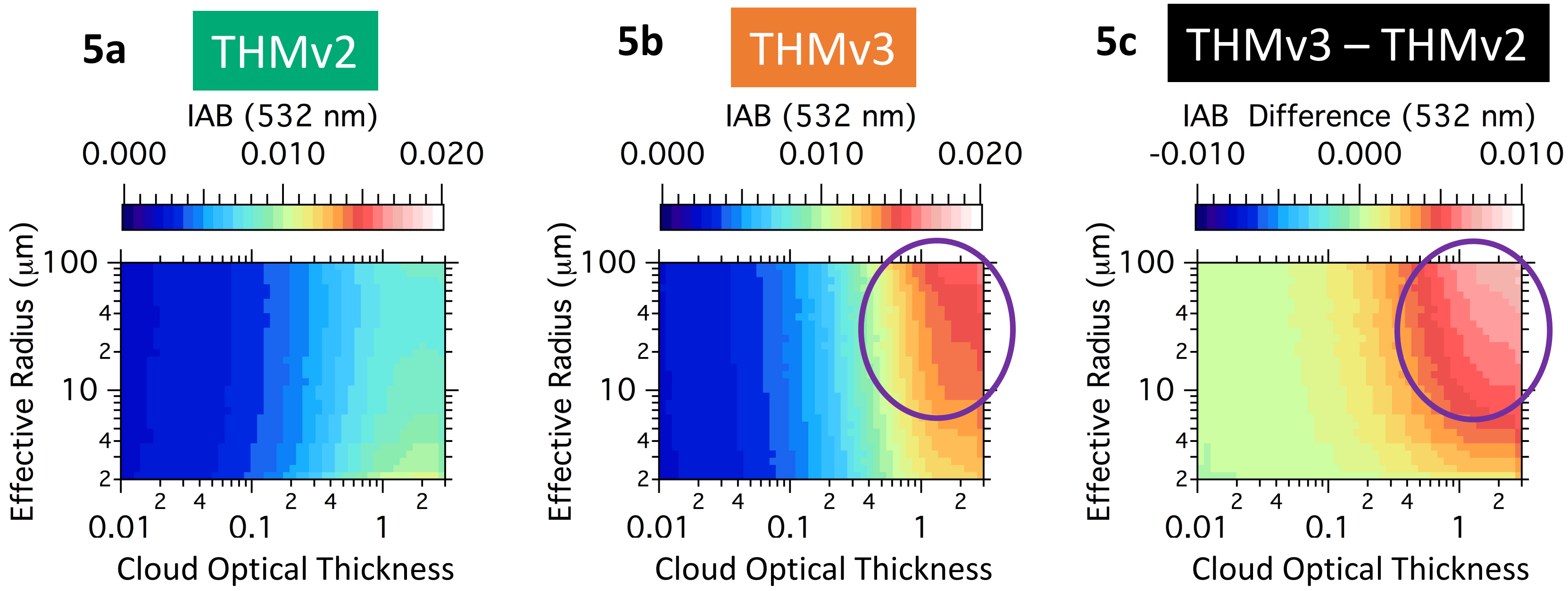

Recap: Preliminary THM Active – Passive Consistency Check

- 532 nm CALIOP/CALIPSO IAB and 8.65, 10.6, and 12.05 µm IIR/CALIPSO Split-Window technique COT retrieval methods utilized to validate active-passive consistencies between the previous and preliminary THM databases.
- New THM showed to achieve active-passive consistency in COT retrievals due to more IAB COT information provided by improved backscattering.

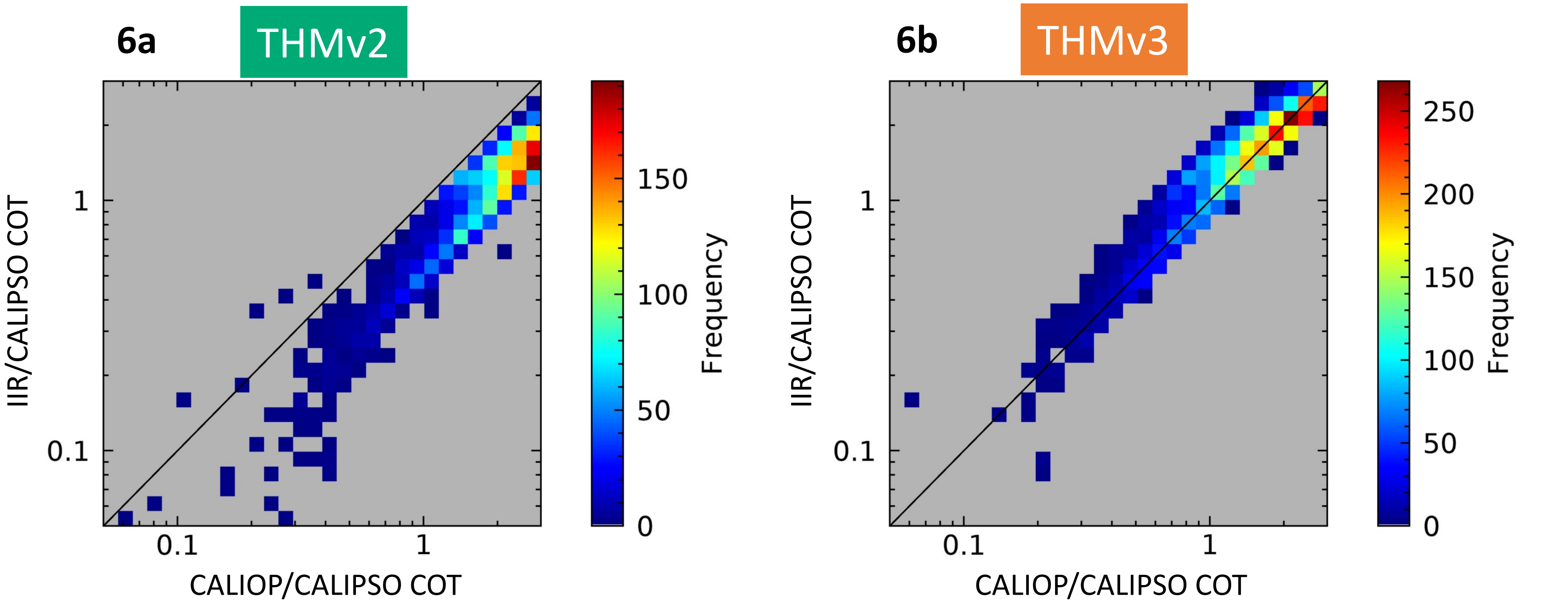

Current Progress: Full Resolution THM Developed

- Full resolution THM database has been developed.
  - 60-particle irregular single column and 20-particle irregular 20-column aggregate ensembles.
  - Volume-projected area equivalent sphere diameter size characterization.
  - Same wavelength and size resolution and range as previous THM.
  - Only IGOM calculations for size parameters > 25.

	New THM (Version 3)
Wavelength	470 bins (0.2 – 200 µm)
Size	189 bins (2.0 – 10000.0 µm)

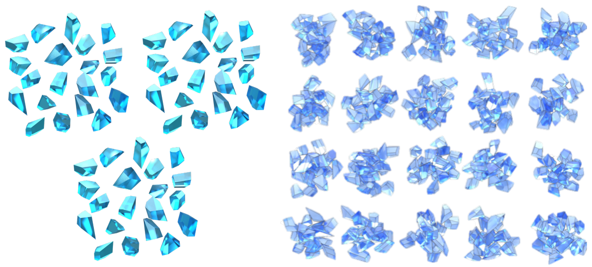

7a THM Computation Methods

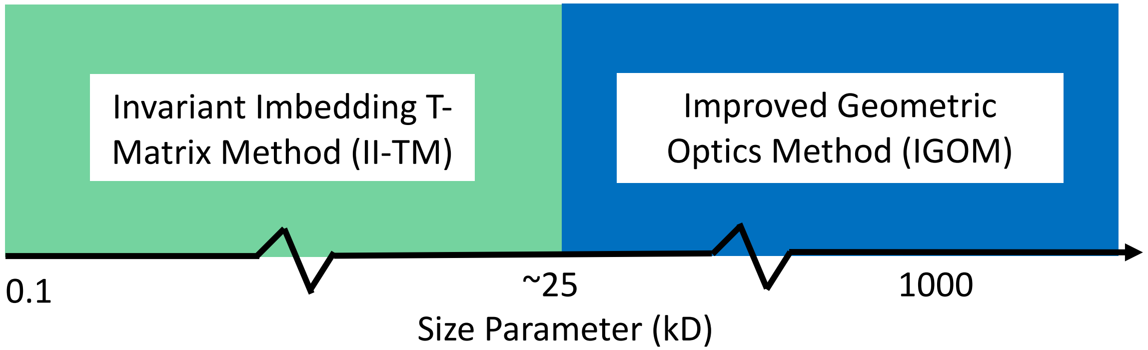

7b

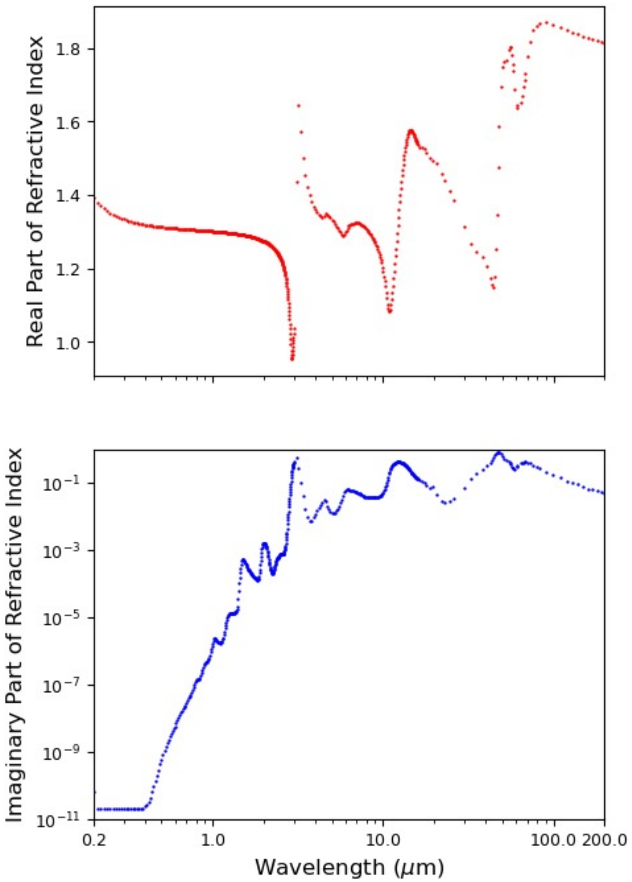

7c

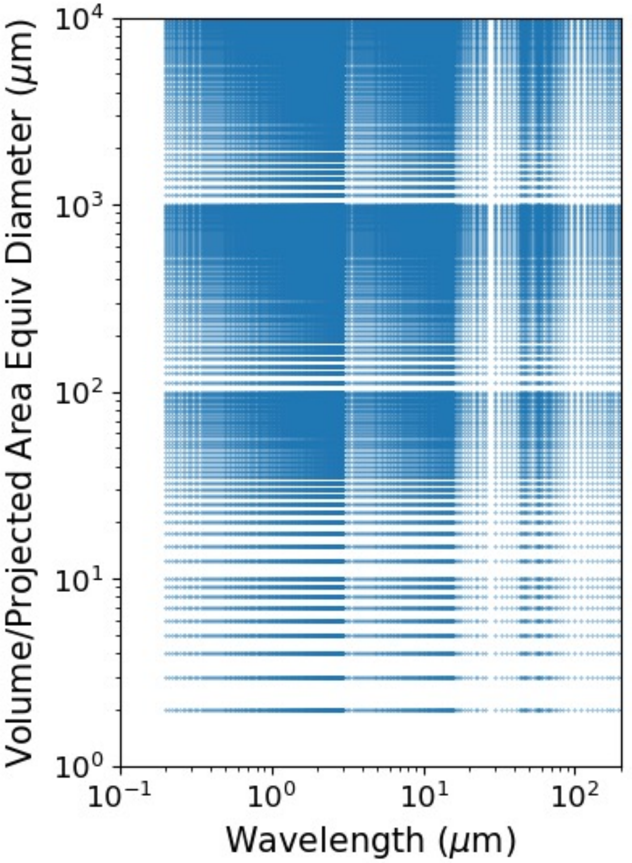

Full Resolution THM Bulk Scattering Property Preview

- Absorptive wavelengths at about 2.9, 11, and 46 µm have significantly low extinction efficiencies, single-scattering albedo (Figure 8a) (due to sharp declines in real part of refractive index).
- Most significant THM version differences in extinction efficiency (Figure 8b).
  - Likely caused by small particle habit change and IITM calculation size parameter limit reduction (THMv2 IITM < 40; THMv3 IITM < 25).

8a THMv3 Bulk Scattering Properties

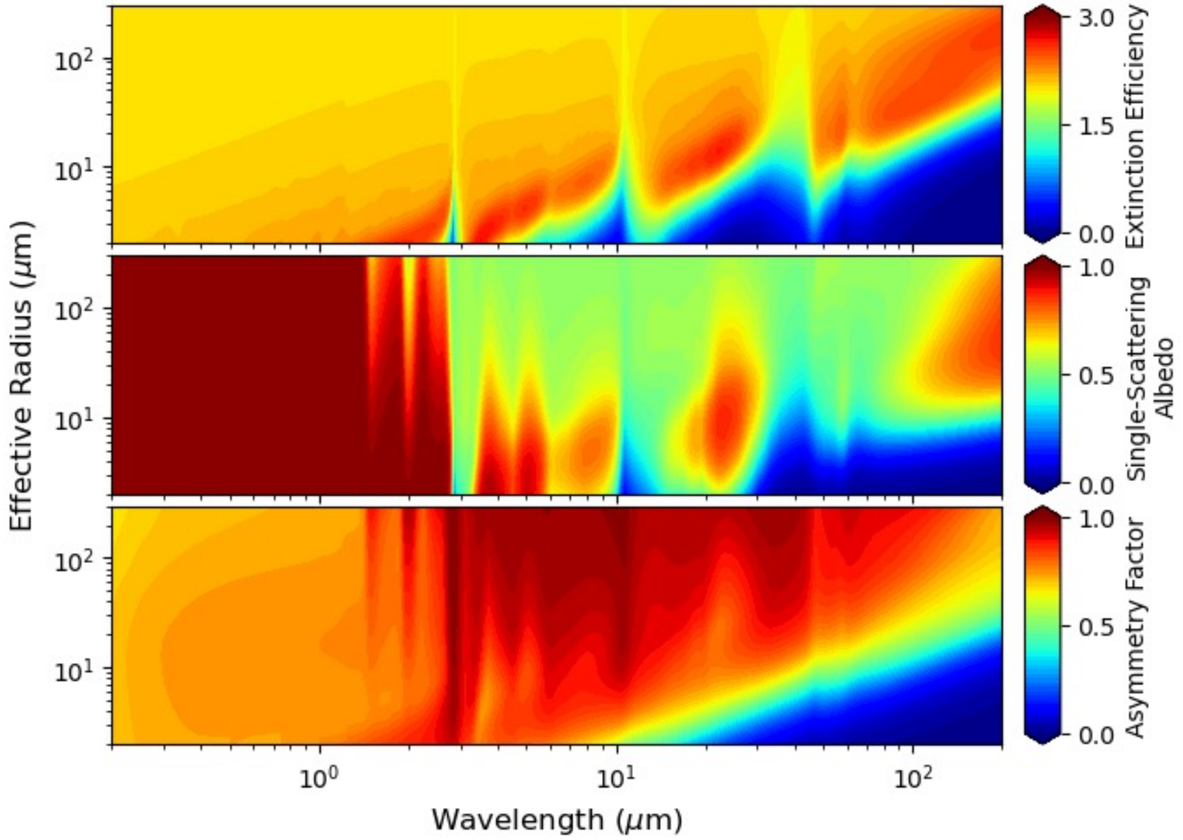

8b THMv3 – THMv2 Scattering Properties

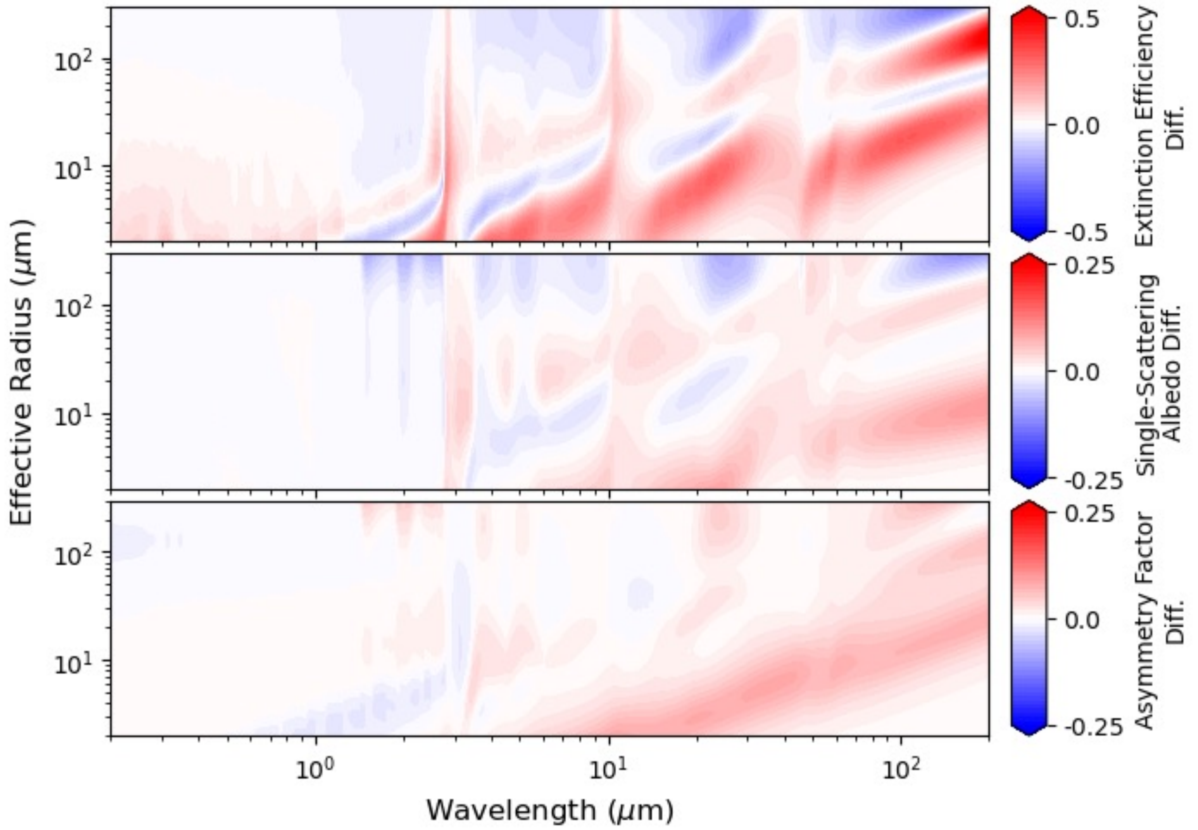

Full Resolution THM Comparison with Previous Version

- Bulk scattering calculations with effective radius eliminate obvious size characterization differences between the two THM versions.
    - Reveals how irregular single column ensemble affected results.
- For small wavelengths (< 4 µm), bulk Q_{ext} (Fig. 9a) for THMv3 less sensitive to absorptive wavelengths.
- THMv3 bulk ω (Fig. 9b) slightly greater than THMv2 throughout nearly all wavelengths (except shortwave).
- THMv3 bulk g (Fig. 9c) slightly less than THMv2 for nearly all wavelengths.
- Overall, distorted single column ensemble more reflective and less sensitive to absorptive wavelengths.

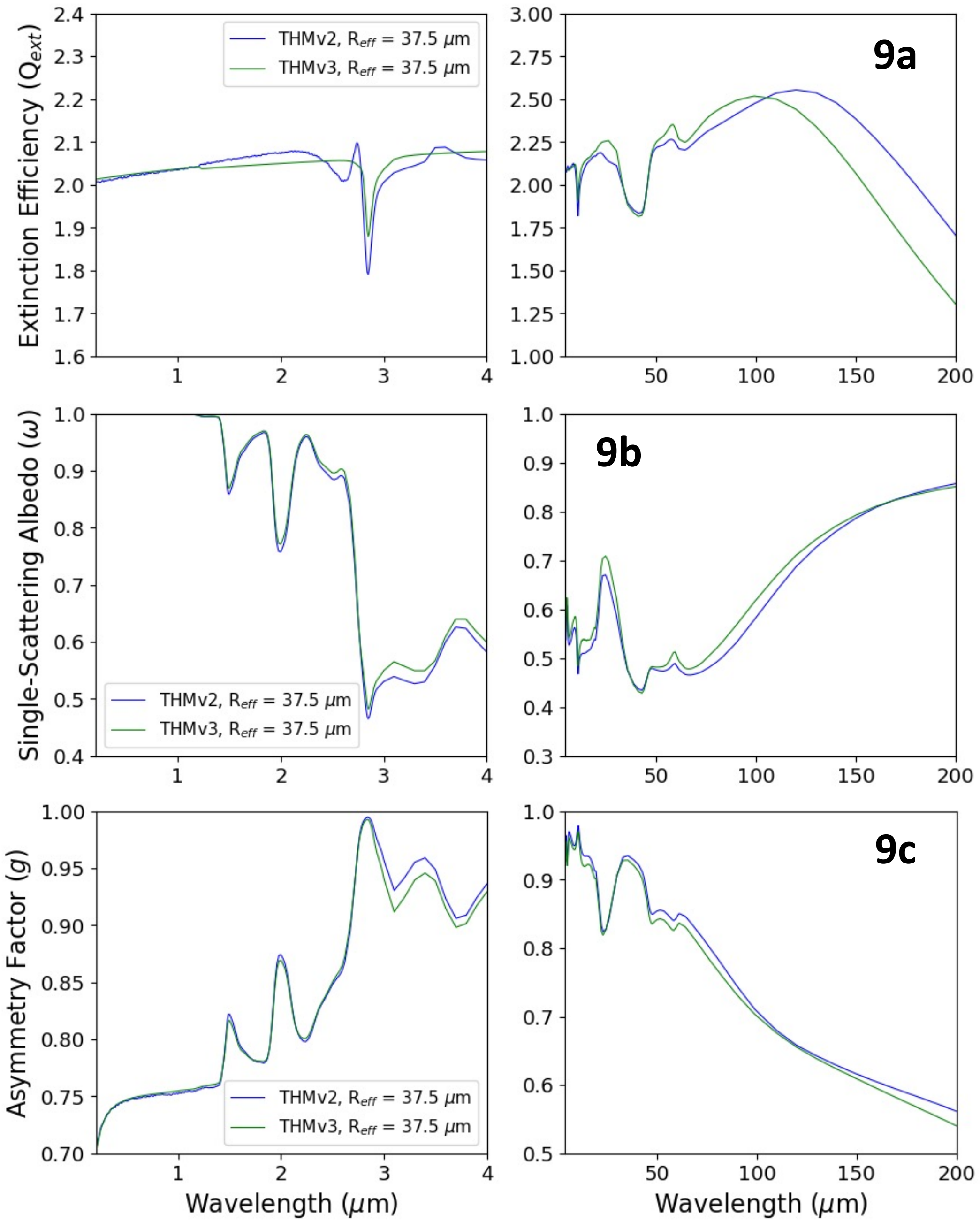

Current Progress: Lidar Version of New THM In Development

- Performing PGOM calculations for the full resolution THM not computationally feasible.
  - Each PGOM calculation takes around 10 min – 1 hour to complete for each wavelength and size.
  - Using backscattering enhancement parameterization like in preliminary THM likely to lead to errors.
- Want to focus on wavelengths commonly used for lidar applications.
  - **355, 532, and 1064 nm** considered for the lidar version of the new THM.
  - Will use PGOM calculations to replace IGOM-calculated backscattering region (160 degrees and greater).

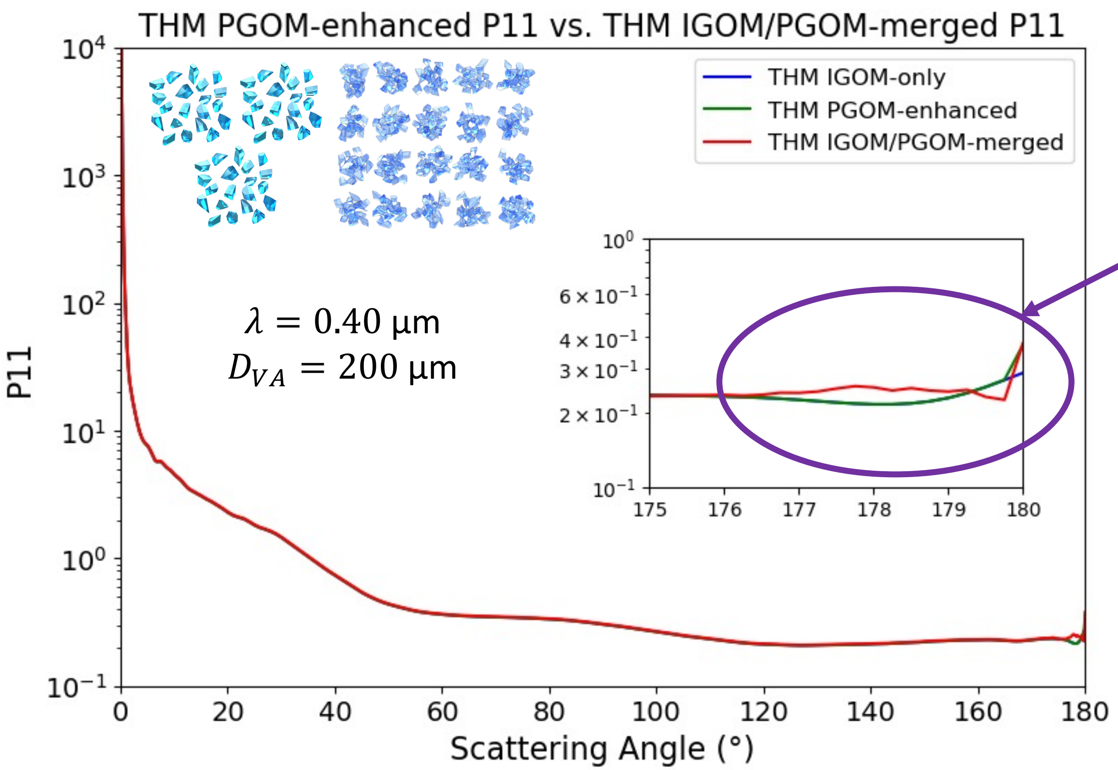

Actual PGOM calculations (red) reveal more backscattering region information than the parameterization (green)

	Lidar THM
Wavelength	3 bins (355, 532, 1064 nm)
Size	189 bins (2.0 – 10000.0 μm)

Preview: 532 nm Lidar Ratio THM vs. Previous THM

- Since the new THM has higher backscattering, the denominator of the lidar ratio will be higher thus reducing the ratio value.
- The THMv3 532 nm lidar ratio ranges from 30 – 40 sr.
  - In agreement with Seifert et al. 2007: lidar ratio of 29 – 33 sr over Indian Ocean.
  - In agreement with Josset et al. 2012: lidar ratio of 33 $\pm$ 5 sr over the global ocean.

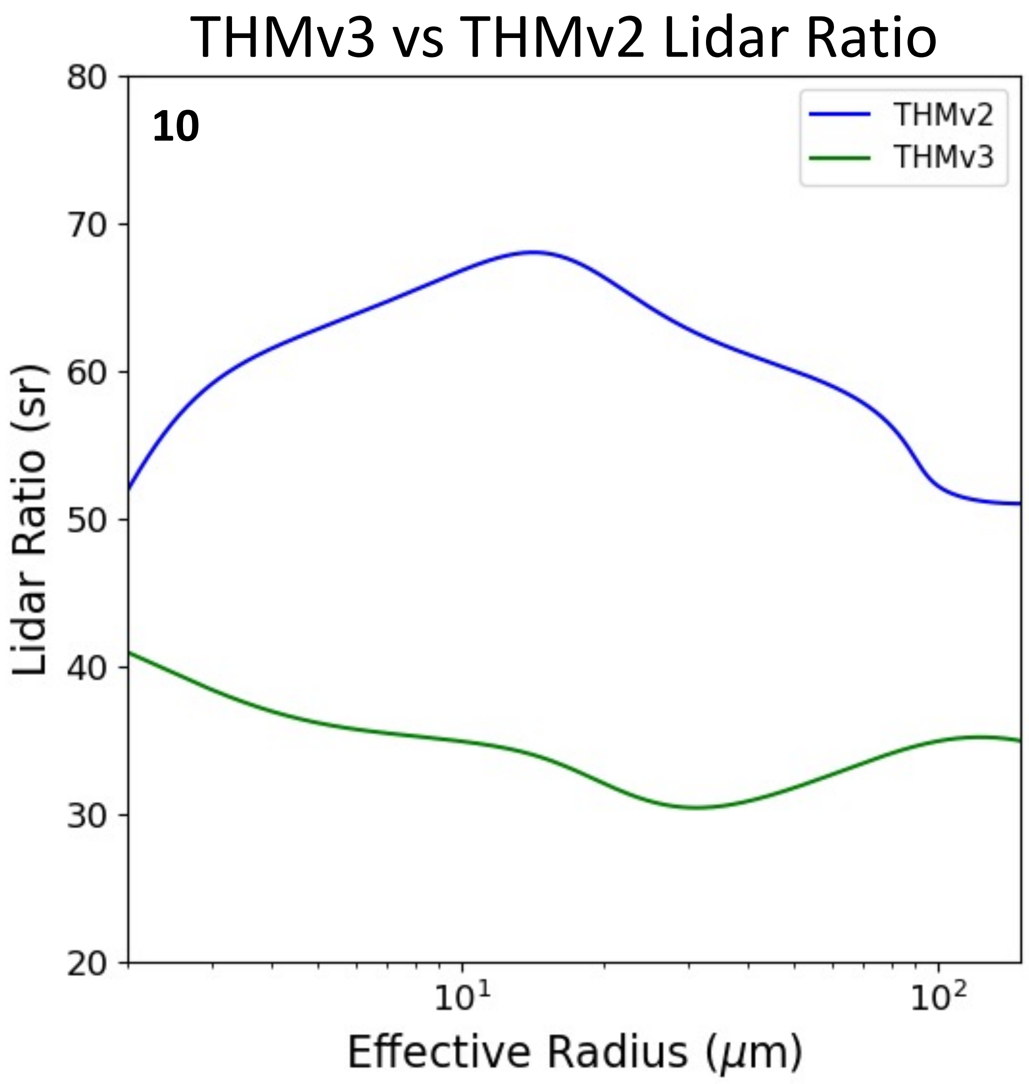

Lidar Ratio

$$S = \frac{4\pi}{\omega_{bulk} P_{11,bulk}(180°)}$$

ω_{bulk}: bulk single-scatting albedo
$P_{11,bulk}$: bulk scattering phase function

Summary

- Successfully developed the full resolution new THM with a new size characterization and particle habit change.
  - Bulk scattering calculations indicate no abnormalities in the new THM.
  - Testing/validation will be conducted using the database in remote sensing applications and broadband radiative transfer simulations.

- Lidar version of the THM is currently in development and will be completed in June.
  - Will demonstrate the improvements in retrievals provided by the accurate PGOM backscattering calculations.
  - Will be compared against the previous THM and a lidar version of the Fu 1996 database that will also have PGOM backscattering calculations.

References

C. Liu, R. L. Panetta, and P. Yang, “The effective equivalence of geometric irregularity and surface roughness in determining particle single-scattering properties,” *Opt. Express* **22**, 23620-23627 (2014a).

D. Josset, J. Pelon, A. Garnier, Y. Hu, M. Vaughan, P. Zhai, R. Kuehn, and P. Lucker, ”Cirrus optical depth and lidar ratio retrieval from combined CALIPSO-CloudSat observations using ocean surface echo,” *J. Geophys. Res.* **117**, D05207.

G. Thompson, P. R. Field, R. M. Rasmussen, and W. D. Hall, “Explicit Forecasts of Winter Precipitation Using an Improved Bulk Microphysics Scheme. Part II: Implementation of a New Snow Parameterization,” *Amer. Metr. Soc.* **136**, 5095-5115 (2008).

N. G. Loeb, P. Yang, F. G. Rose, G. Hong, S. Sun-Mack, P. Minnis, S. Kato, S. Ham, W. L. Smith Jr., S. Hioki, and G. Tang, “Impact of Ice Cloud Microphysics on Satellite Cloud Retrievals and Broadband Flux Radiative Transfer Model Calculations,” *J. Clim*. **31**, 1851-1864 (2018).

J. Ding, P. Yang, R. E. Holz, S. Platnick, K. G. Meyer, M. A. Vaughan, Y. Hu, and M. D. King, “Ice cloud backscatter study and comparison with CALIPSO and MODIS satellite data,” *Opt. Express* **24**, 620-636 (2016).

M. Saito, H. Iwabuchi, P. Yang, G. Tang, M. D. King, and M. Sekiguchi, “Ice particle morphology and microphysical properties of cirrus clouds inferred from combined CALIOP-IIR measurements,” *J. Geophys. Res*. **122**, (2017).

P. Seifart, A. Ansmann, D. Muller, U. Wandinger, D. Althausen, A. J. Heymsfield, S. T. Massie, and C. Schmitt, “Cirrus optical properties observed with lidar, radiosonde, and satellite over the tropical Indian Ocean during the aerosol-polluted northeast and clean maritime southwest monsoon,” *J. Geophys. Res.* **112**, D17205.

P. Yang and K. N. Liou, “Geometric-optics-integral-equation method for light scattering by non-spherical ice particles,” *Appl. Opt.* **35**, 6568-6584 (1996).

T. C. Grenfell and S. G. Warren, “Representation of a nonspherical ice particle by a collection of independent spheres for scattering and absorption of radiation,” *J. Geophys. Res.* **104**, 31697-31709 (1999).

T. Inoue, “A cloud type classification with NOAA 7 split-window measurements,” *J. Geophys. Res.* **92**, 3991-4000 (1987).